Available online at www.sciencedirect.com
SCIENCE DIRECT®
Surface and Coatings Technology 179 (2004) 119–123
SURFACE & COATINGS TECHNOLOGY
www.elsevier.com/locate/surfcoat

On the kinetics of plasma nitriding a martensitic stainless steel type AISI 420

Carlos E. Pinedo[a,*], Waldemar A. Monteiro[b]

[a]*University of Mogi das Cruzes, Technological Research Centre, Av. Cândido Xavier de Almeida Souza 200, Mogi das Cruzes, SP 08780-210, Brazil*
[b]*Center of Materials Science and Technology, Energetic and Nuclear Research Institute, IPEN-CCTM, Cidade Universitária Armando Salles de Oliveira, Travessa R–400, São Paulo, SP 05508-970, Brazil*

Received 20 May 2002; accepted in revised form 22 June 2003

Abstract

Plasma nitriding was employed to treat martensitic stainless steel type AISI 420. The ability to remove the passive film from the surface is an important advantage in this process in order to guarantee a homogeneous surface treatment. The resulting nitrided surface shows the presence of a compound layer and a diffusion zone. The interface between the diffusion zone and the substrate is flat, as a consequence of the high chromium content on the alloy. The precipitation of chromium nitrides is also responsible for the high levels of hardening obtained. A value up to 1350 HV 0.025 constituting a maximum hardness was obtained. Diffusion depth increases with an increase of the nitriding temperature as measured by optical microscopy and verified by the hardness profiles. Calculated diffusion coefficients of nitrogen were very low compared to the data for alpha iron, and allow calculation of the Arrhenius behaviour during the process.

Keywords: Plasma nitriding; Morphology; Kinetics; Martensitic stainless steel; Hardening

1. Introduction

Nitriding is a thermochemical surface treatment widely used to treat steels and alloys. The main advantages of this process are the improvement of wear and frictional properties, corrosion, and fatigue [1]. Plasma nitriding [2–4] is one of the most versatile nitriding processes with many advantages over the conventional salt-bath and gas nitriding. The control of the metallurgical properties of the nitrided surface is the most important advantage of the plasma nitriding process, especially for high alloy steels. Nowadays, duplex and hybrid layers are gaining in importance, requiring prior nitriding of the substrate. For the development of these processes, the understanding of the plasma nitriding behavior of the martensitic stainless steel is a very important step.

The aim of the present investigation is to study nitriding characteristics of the high-alloyed chromium steel. As pointed out by literature [5,6], the presence of alloying elements, particularly nitrides forming, have a strong influence on the hardening, morphology and kinetics characteristics of the nitrided surface. The influence of nitride forming elements is dependent on the degree of interaction with nitrogen. Elements like Al and Ti have a strong interaction with nitrogen, while the interaction of Cr is dependent on the alloy content on steel. It is considered that chromium content below 5.6 mass percent has intermediate interaction behaviour, and for higher contents, this element presents strong interaction characteristics.

Martensitic stainless steels are widely used as molds for plastic injection and glass molding, cutting tools, structural parts, automotive components, surgical and dental instruments, where wear and corrosion properties are also required. In a previous work, the plasma nitriding of the steel type AISI 440B was studied, allowing us to best understand the hardening character-

*Corresponding author. Tel.: +55-11-4798-7229; fax: +55-11-4799-2069.
E-mail address: pinedo@umc.br (C.E. Pinedo).

0257-8972/04/$ - see front matter © 2003 Elsevier B.V. All rights reserved.
doi:10.1016/S0257-8972(03)00853-3

istics and selective nitriding on properties and fabrication route of piston rings in order to increase the performance and safe costs [7]. Results for the type AISI 420, plasma nitrided at temperatures from near 480 to 560 °C, showed that the hardening effect is high enough to increase the hardness on the nitrided case from 380 HV up to 1350 HV, and a planar nitriding interface growth mode [8–10]. In the present article, we intend to best investigate and understand the kinetics and the morphology of the nitrided case.

2. Experimental methods

A wrought martensitic stainless steel type 420 was received in the annealed round bar condition. The chemical composition in mass percent was Fe-0.40C–13.5Cr–0.25V. In the as received annealed state, the microstructure was composed of a ferritic matrix with a secondary $M_{23}C_6$ carbide dispersion. Before nitriding, the samples were cut transverse from the original bar obtaining 5 mm thick samples. All the samples were quenched in oil, from austenitizing temperature of 1025 °C, and double tempered at 580 °C for 36.0 HRC substrate hardness, to avoid the substrate hardness loss after nitriding.

The equipment used in the experimental work was a hot wall/direct current glow-discharge furnace, from ELTROPULS GmbH, with a vacuum chamber: 450 mm diameter and 800-mm high. A computer system controls simultaneously the most important nitriding parameters such as: gas mixture, pressure, voltage, temperature and time. During thermochemical treatment, before the nitriding step, the samples were sputtered in high-density pure hydrogen plasma to remove the passive oxide film from the surface. The nitriding temperatures were 480, 500, 520, 540 and 560 °C, with constant time and gas mixture composition. The nitriding time was 4 h and the gas mixture ratio was $N_2/H_2=3/1$. The selected process parameters upon the nitriding step were: voltage: 470 V, pulse duration: 50 μs, pulse repetition: 150 μs and pressure: 250 Pa. Two thermocouples were used embedded in the samples in order to best guarantee the treatment temperature accuracy.

Nitrided surface microstructure was observed using the optical (OM) and scanning electron microscopy (SEM), after etching by Nital 4%. The nitriding depth was measured by the OM using an image analysis system; LEO 500 MC. Microhardness measurements were performed using Vickers measurements with 25 g load. Additionally, X-ray diffractometry (XRD) analysis were performed on the compound layer and diffusion zone using CuK_α radiation ($\lambda=0.1542$ nm) in conventional $\theta/2\theta$ Bragg–Brentano symmetric geometry. Additionally, analysis by energy dispersive electron spectroscopy (EDS) was used for the characterization of nitrogen distribution across the nitrided case. The

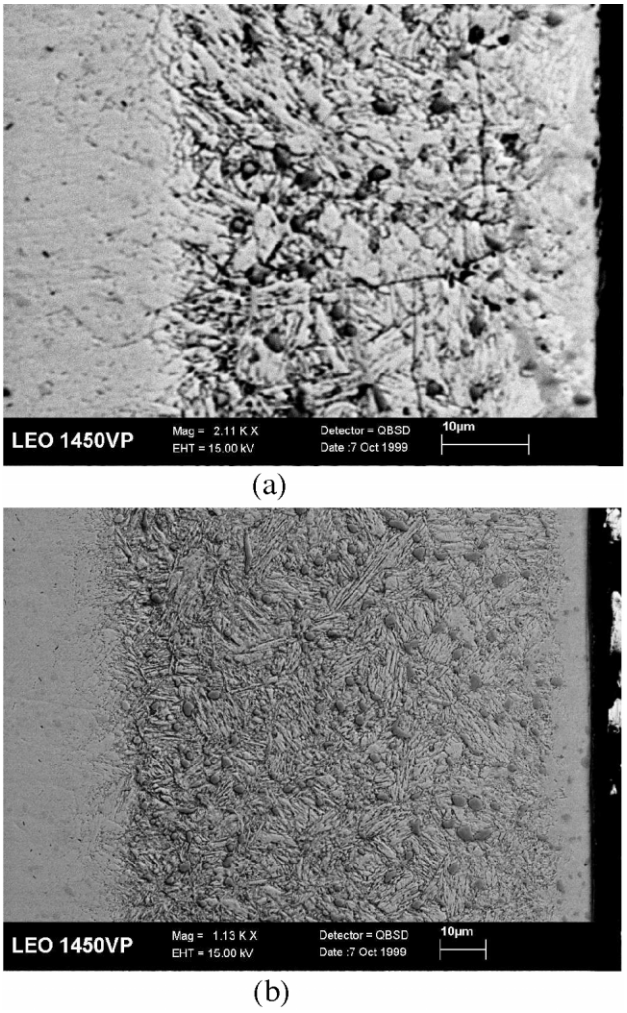

Fig. 1. Surface microstructures observed in SEM after nitriding at 480 °C (a) and 560 °C (b). Nital 4%.

case depth at each nitriding temperature allows us to determine the diffusion coefficient of nitrogen on the matrix. The activation energy for diffusion and the frequency factor were evaluated by measuring the evolution of the nitriding depth as a function of temperature, assuming that the diffusion coefficient obeys Arrhenius behaviour.

3. Results and discussion

Fig. 1 shows the surface microstructures after the nitriding treatments. For all the nitriding temperatures, the nitrided case is composed of an upper compound layer and a lower diffusion zone. At the present work, the decrease of nitriding temperature up to 480 °C was not effective to avoid the compound layer formation, as a result of the high nitrogen potential used on the nitriding gas mixture. Similar results were obtained after plasma nitriding martensitic stainless steel type AISI 410 (0.1%C–12%Cr) at temperatures higher than 450

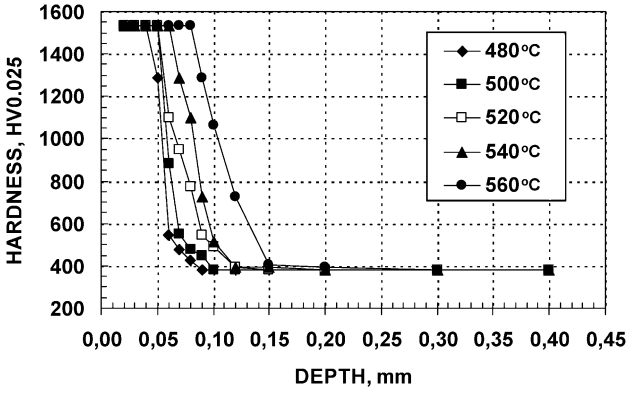

Fig. 2. Hardness profiles determined for each nitriding temperature.

°C and high nitrogen potential on the gas mixture [11,12]. Previous work on steel type AISI 440B (0.90%C–18%Cr) [7] showed that the compound layer is avoided after nitriding at 520 °C, for 4 h with a gas mixture containing 50%N_2. For both AISI 410 [12] and AISI 420 [13] steels, on lower nitriding temperature, the compound layer and the continuous sub-microscopic nitrides precipitation on diffusion zone are not present. According to the most recent work from Kim [13], when the nitriding temperature is close to 400 °C the diffusion zone is composed by a so-called 'expanded martensite', similar to the expanded austenite [γ_N] verified on low temperature nitriding austenitic stainless steels [14,15].

Upon increasing of the nitriding temperature, there was a thickening of the nitriding case, compound layer and diffusion zone. Regarding the diffusion zone there was no grain boundaries of nitrides network, and a well-defined planar interface between the diffusion zone and the substrate is observed for all nitriding temperatures. The hardness profiles, Fig. 2, shows a strong hardening effect by nitriding, due to the precipitation of a fine and homogeneous γ'-Fe_4N, ε-$Fe_{2-3}N$ and CrN nitrides [10–12,16] on diffusion zone. The main characteristic of the hardness profiles was a sharp decrease after the maximum hardness horizontal plateau; the hardness profiles were coincident in shape with the nitrogen profile across the nitrided case, and were closely related to the nitriding mechanism. Using the EDS spectra Fig. 3, a clear difference can be seen between the nitrogen content measured at a fixed depth of 80 μm, after nitriding at 480 and 560 °C. Marchev [12] results for ion-nitriding of the grade AISI 410, showed flat horizontal hardening profiles for nitriding at 510 °C and gradual for nitriding at 400 °C, suggesting that different nitriding mechanism for the diffusion zone growth are present at low and high nitriding temperature.

For the compound layer, the X-ray diffraction pattern in Fig. 4 shows that γ'-Fe_4N, ε-$Fe_{2-3}N$ and CrN nitrides are present. These results are in accordance with those,

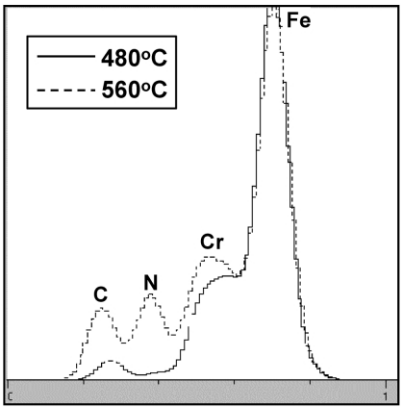

Fig. 3. X-ray diffraction pattern for the compound layer after nitriding at 560 °C.

recently presented by Borgioli and co-workers [16,17], but two extra peaks were observed in this study for 2θ positions of 79.01° and 77.42°, corresponding to the γ'-Fe_4N and CrN nitrides, respectively. The analysis of the four CrN peaks allow us to determine the lattice parameter for this cubic nitride as being 0.412 ± 0.002 nm, close to the value presented by *JCPDS-ICDD*© data files, 0.414 nm.

From the nitriding depth data, the diffusion coefficient of nitrogen was calculated for each temperature using the equation $x = \sqrt{D_N t}$, where 'x' is the nitriding depth,

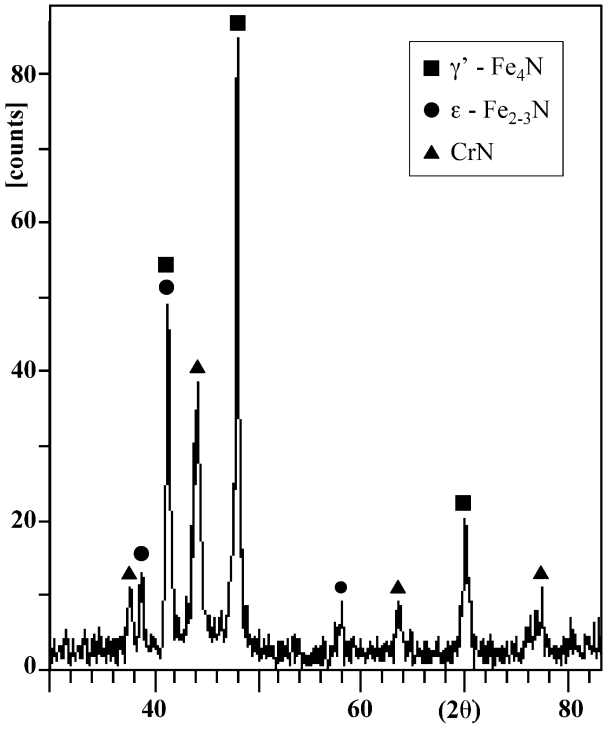

Fig. 4. EDS spectrum for the nitriding in two different nitriding temperatures, measured at 80 μm depth.

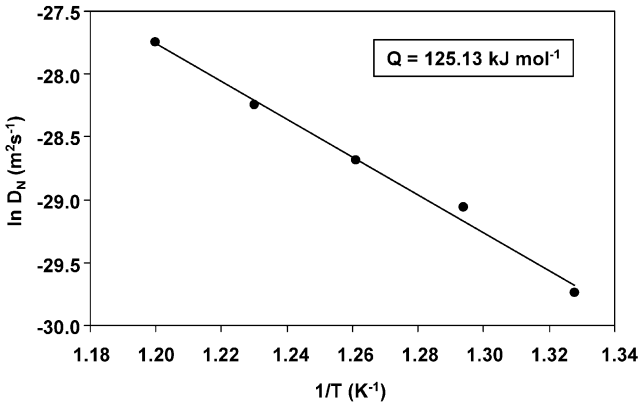

Fig. 5. Determination of the activation energy using linear regression.

'D_N' is the effective diffusion coefficient of nitrogen and 't' is the nitriding time. By using calculates of D_N data and considering Arrhenius-type behaviour; the activation energy for nitrogen diffusion was calculated using linear regression [18,19], as shown in Fig. 5. From the calculated activation energy the effective diffusion coefficient of nitrogen on plasma nitriding such as high chromium steel may be described by the equation below:

$$D_N = 6.066 \times 10^{-05} \exp\left(\frac{-125.1}{RT}\right).$$

Some nitriding mechanisms have been presented recently on plasma nitriding of martensitic stainless steel [7–13], and allow us to support the presented results. According to Kim [13], the activation energy for plasma nitriding the steel AISI 420 at 400 °C is 33.43 kJ/mol. However, at this temperature the volume diffusion of nitrogen on the matrix is the unique operating processes, expanding the martensite lattice, but without any nitride precipitation. Comparing to the present results, the need of nitrides precipitation on the temperatures used in this work is the reason for the highest activation energy value. On high temperature nitriding, where nitrides precipitation are ready to occur [7–12], the growth of the nitrided case is affected by the precipitation reactions at the moving interface, affecting the value of the calculated activation energy. In this case, it is verified that the nitrides precipitation delays the process and increase the activation energy.

Markev [12] shows the nitrogen compositional profiles across the nitrided interface for the steel type AISI 410 after low (400 °C), and high (510 °C) nitriding temperature. At 510 °C, the compositional profile is horizontal, step-shaped; while at 400 °C the nitrogen profile exhibit a more gradual decrease. In both case the hardness profiles follow the compositional profile, suggesting a different nitriding mechanism. As pointed out by Möller and co-workers for the ion nitriding of aluminium [20], the activation energy reflects not only the need for nitrogen diffusion across the nitrided case, but also the need for chromium diffusion from under laying bulk positions to the nitriding interface for the CrN nitride precipitation.

4. Conclusions

For all the nitriding temperatures, the nitrided surface is composed of the compound layer and the diffusion zone, even at low temperatures, as a result of the high nitrogen potential on the gas mixture. The diffusion zone is free from intergranular nitrides and the interface between the diffusion zone and the substrate is flat.

The maximum nitriding surface hardness was up to 1500 HV 0.025. The hardness profiles show a step-shaped decrease from the maximum hardness to the core hardness. This behaviour is a consequence of the complex nitriding reactions that take place at the interface, and reflects the nitrogen compositional profile across the nitrided case.

The calculated effective diffusion coefficient calculated herein is the result of both nitrogen volume diffusion and nitrides precipitation reactions at the interface. For the same reason, the activation energy for nitriding the high chromium steel is two times higher than that for the pure iron, and four times higher than for the steel grade 420 nitrided at low temperature. The calculated kinetic parameters, D_N and Q, were affected by the complex reactions that took place at the interface, and cannot be assumed solely as a function of the volume diffusion of nitrogen on the tempered martensite matrix, but more controlled by the precipitation reactions at the nitriding interface.

References

[1] T. Sun, T. Bell, Mater. Sci. Eng. 140 (1991) 419–434.
[2] B. Edenhofer, Heat Treatment Metals Part 1 (1974) 23–28.
[3] K.-T. Rie, Surf. Coat. Technol. 112 (1999) 56–62.
[4] M. Berg, C.V. Budtz-Jørgensen, H. Reitz, K.O. Schweitz, J. Chevallier, P. Kringhøj, et al., Surf. Coat. Technol. 124 (2000) 25–31.
[5] D.H. Jack, Proceedings of the Heat Treatment 1973, London/UK, 1973, pp. 39–50.
[6] J. Lightfoot, D.H. Jack, Proceedings of the Heat Treatment 1973, London/UK, 1973, pp. 59–65.
[7] C.E. Pinedo, Mater. Des. 24 (2003) 131–135.
[8] C.E. Pinedo, Ph.D. Thesis, Energetic and Nuclear Research Institute–São Paulo University, São Paulo, SP, Brazil, 2000.
[9] C.E. Pinedo, W.A. Monteiro, Acta Micros. 1 (2001) 315–316.
[10] C.E. Pinedo, W.A. Monteiro, J. Mater. Sci. Lett. 20 (2001) 147–149.
[11] E. Stagno, M.R. Pinasco, M.G. Ienco, G. Palombarini, G.F. Bocchini, J. Alloy Compd. 247 (1997) 172–179.
[12] K. Marchev, C.V. Cooper, B.C. Giessen, Surf. Coat. Technol. 99 (1998) 229–233.
[13] S.K. Kim, J.S. Yoo, J.M. Priest, M.P. Fewell, Surf. Coat. Technol. 164 (2003) 380–385.

[14] M.P. Fewell, J.M. Priest, M.J. Baldwin, G.A. Collins, K.T. Short, Surf. Coat. Technol. 131 (2000) 284–290.
[15] M.P. Fewell, D.R.G. Mitchell, J.M. Priest, K.T. Short, G.A. Collins, Surf. Coat. Technol. 131 (2000) 300–306.
[16] F. Bogioli, E. Galvanetto, T. Bacci, G. Pradelli, Surf. Coat. Technol. 149 (2002) 192–197.
[17] T. Bacci, F. Borgioli, E. Galvanetto, G. Pradelli, Surf. Coat. Technol. 139 (2001) 251–256.
[18] L. Torchane, P. Bilger, J. Dulcy, M. Gantois, Metall. Mater. Trans. 27A (1996) 1823–1835.
[19] M.A.J. Somers, E.J. Mittemeijer, Metall. Mater. Trans. 26A (1995) 57–74.
[20] W. Möller, S. Parascandola, T. Telbizova, R. Günzel, E. Richter, Surf. Coat. Technol. 136 (2001) 73–79.